Journal of Applied and Natural Science
18(1), 250 - 265 (2026)
ISSN : 0974-9411 (Print), 2231-5209 (Online)
journals.ansfoundation.org

Research Article

Assessing neotectonic activity in the Ladhiya River basin, Eastern Kumaun Himalaya using Index of relative active tectonics (IRAT)

Mohd. Nazish Khan
Department of Physical Geography and Natural Resources, Samarkand State University, Uzbekistan
M. Suhail
Center of Applied Remote Sensing and GIS Applications, Samarkand State University, Uzbekistan
Dilawez Ali
Department of Geology, Samarkand State University, Uzbekistan
Mohammad Faizan
Department of Geology, Aligarh Muslim University, Aligarh, India
Samyayev Anvar Kadirovich
Pedagogical professional development center of Samarkand Region, Samarkand, , Uzbekistan
Egamberdiev Asamberdi
National University of Uzbekistan named after Mirzo Ulughbek, Tashkent, Uzbekistan

*Corresponding author. E-mail: dilawezali007@gmail.com

Article Info
https://doi.org/10.31018/jans.v18i1.6940
Received: July 19, 2025
Revised: February 08, 2026
Accepted: February 23, 2026

How to Cite
Khan, M. N. *et al.* (2026). Assessing neotectonic activity in the Ladhiya River basin, Eastern Kumaun Himalaya using Index of relative active tectonics (IRAT). *Journal of Applied and Natural Science*, 18(1), 250 - 265. https://doi.org/10.31018/jans.v18i1.6940

Abstract
The Ladhiya River, flowing from west to east, drains the Lesser Himalayan zone and intersects several active faults, thrusts, and lithotectonic units before merging with the Kali River at Chuki Gaon. The present study aimed to evaluate the effectiveness of geomorphic indices in assessing neotectonic activity within the Ladhiya River Basin, located in the Eastern Kumaun region of the Himalayas. Utilizing Advanced Spaceborne Thermal Emission and Reflection Radiometer (ASTER) DEM data, the total 7 watershed were delineated at a 50,000 threshold and the drainage network at a 100 threshold for detailed processing and analysis. The study focused on determining the relative tectonic activity of the Ladhiya River Basin by employing the Index of Relative Active Tectonics (IRAT), which incorporates various geomorphic indices such as Drainage Density (Dd), Drainage Texture (Dt), Hypsometric Integral (HI), Bifurcation Ratio (Br), Asymmetry Factor (Af), Valley Floor Width to Height Ratio (Vf), Stream Length Gradient (SL), and Mean Stream Length (MSL). These indices were categorized into three classes to rank each sub-basin, ultimately deriving the IRAT. The sub-basins situated on the left bank of the Ladhiya River exhibited a pronounced influence of neotectonic activity. This was particularly evident in the stream length gradient values, wherein the Dholigaon, Bigrakot, and Khatoli sub-basins display relatively high magnitudes, indicating active tectonic adjustments within these areas. The IRAT results show that areas near the trunk stream experience strong denudation, while regions farther away exhibit tectonic uplift, providing a clear picture of neotectonic activity in the Ladhiya River Basin.

Keywords: ASTER, Active tectonics, Index of relative active tectonics (IRAT) , Ladhiya River, Morphotectonics

INTRODUCTION

The Himalayan orogeny resulted from the collision between the Indian and Eurasian continental plates approximately 65 million years ago, during the Eocene epoch (Gansser, 1964; Dewey and Bird, 1970; McKenzie and Sclater, 1971; Molnar and Tapponnier, 1975). This collision led to the formation of three major north-dipping thrust zones—the Main Central Thrust (MCT), Main Boundary Thrust (MBT), and Himalayan Frontal Thrust (HFT)—which become progressively younger from north to south (DeCelles *et al*., 2000). These thrusts are interconnected by various tectonic structures and geomorphic features, continuously shifting

southward due to collision and convergence (Kalpana *et al*., 2023; Khan and Govil, 2023; Khan *et al*., 2024). Additionally, the Himalaya is undergoing constant evolution, evident in active faults and thrusts, rising peaks, fault scarps, V-shaped canyons, shutter ridges, offset streams, knick points, waterfalls, and its dramatically varied landscape, including the 8,848-meter-high Mount Everest (Husson *et al*., 2014).

The Lesser Himalayan sequence is divided into two distinct units: the Inner Lesser Himalaya and the Outer Lesser Himalaya (Valdiya, 1980a, 1980b; Pant *et al*., 2012; Farooq *et al*., 2015). These units are separated by the North Almora Thrust, which serves as a key structural boundary (Valdiya, 1980a, 1980b; Srivastava and Mitra, 1994; Ahmad *et al*., 2000; DeCelles *et al*., 2001; Richards *et al*., 2005; Kothyari and Luirei, 2016; Khan and Govil, 2023). Tectonic activity along faults and thrusts significantly influences the geomorphic evolution of drainage basins across the Himalayas. The region's dynamic and youthful topography makes it an excellent natural laboratory for investigating basin morphometry and neotectonic processes, as reflected in extensive research on its evolving landscape (Tapponnier *et al*., 2001; Beaumont *et al*., 2001; Farooq *et al*., 2015; Kothyari and Luirei, 2016; Pant and Singh, 2017; Kothyari *et al*., 2017, 2019, 2020; Khan and Govil, 2023).

Tectonic activity, primarily along faults and thrusts, plays a crucial role in shaping the geomorphic evolution of drainage basins throughout the Himalayas. The region's youthful and dynamic landscape provides an ideal setting for studying basin morphometry and neotectonics, as evidenced by extensive research on its evolving topography (Harrison *et al*., 1992; Burtman and Molnar, 1993; Royden *et al*., 1997; Ramstein *et al*., 1997; Tapponnier *et al*., 2001; Beaumont *et al*., 2001; Agarwal *et al*., 2012; Farooq *et al*., 2015; Kothyari and Luirei, 2016; Pant and Singh, 2017; Kothyari *et al*., 2017, 2019, 2020; Luirei *et al*., 2022; Khan and Govil, 2023; Khan *et al*., 2024).

Morphotectonic indices serve as valuable tools for evaluating active tectonics. These indices illustrate how landscape evolution is influenced by the interaction of tectonic activity, surface geological processes, climate change, rock resistance, and structural features. Ladhiya river basin was selected for the current active tectonic evaluation and considered a suitable site for assessing tectonic activity. The drainage network is the product of lithological and tectonic interplay and is considered a reliable indicator of active tectonics. Morphometric analysis of drainage basins provides insights into the steady-state conditions of rocks during active deformation (Seeber and Gornitz, 1983; Ouchi, 1985; Marple and Talwani, 1993; Koons, 1995; Hallet and Molnar, 2001; Thomson *et al*., 2001; Arisco *et al*., 2006; Farooq *et al*., 2015; Khan and Govil, 2023).

The present study aimed to focuses on the quantification of morphotectonic indicators including Drainage Density (Dd), Drainage Texture (Dt), Hypsometric Integral (HI), Bifurcation Ratio (Br), Asymmetry Factor (AF), Valley Floor Width to Height Ratio (Vf), Stream Length Gradient (SL), and Mean Stream Length (MSL) through geospatial technology, helps in providing vital information for computing these indices.

MATERIALS AND METHODS

Study area

The Ladhiya River Basin lies between 79° 40'E to 80° 29'N and 30°N, is located in the eastern Kumaun Himalaya. It forms the major drainage system of the area and originated at North Gola Range Mountains. It travels 77.3 km in the east to west direction before confluencing with the Kali River. The Kali River becomes the Sharda River before reaching Tanakpur. It displays a mosaic of geomorphic features including deep gorges, faults scarps, dendritic to sub-dendritic drainage systems, angular tributaries, and abrupt changes in the course of the river (Fig. 1).

The route from north to south traverses across Bhabhar Formation, Siwalik Group of rocks, Bhimtal Quartzites and Almora Crystallines. The geological formations are separated by major tectonic planes viz., the Himalayan Frontal Faults (HFF), Main Boundary Fault (MBF) and South Almora Thrust (SAT). Out of the entire Himalayan terrain, the outer Himalaya is believed to show excellent signatures of active tectonics. The Main Boundary Thrust (MBT), which separates the Outer and Lesser Himalayas, has documented evidence of recent tectonic activity (Khan and Govil, 2023).

Specifically, the Ladhiya River Basin comprises sedimentary and metasedimentary rocks including slates, phyllites, quartzites, and limestones. These formations undergone varying degree of metamorphism and deformation due to ongoing convergence between Indian and Eurasian plates.

The tectonic features play pivotal roles in defining the basin's geology and exhibits prominent structural features such as folds, faults, and thrusts. The Main Boundary Thrust (MBT) is a significant feature in the close proximity to the basin, marking the boundary between the Lesser Himalaya and the Susb-Himalaya. The alignment and orientation of these structures influence the river's course and evolution of the river basin.

Data and methodology

In this study, the morphotectonic analysis of the Ladhiya River Basin was conducted using satellite data combined with virtual investigations of high-resolution data. The Advanced Spaceborne Thermal Emission and Reflection Radiometer (ASTER) data were utilized to generate a Digital Elevation Model (DEM), which was fur-

Table 1. Showing the morphotectonic parameters and their methods of calculation

Aspects	Morphometric indices	Formula	Reference
Linear	Drainage density (Dd)	Dd = Lu/ A where Lu is the length of the stream of all orders and A is the area of the basin.	Horton, 1932
	Drainage texture (Dt)	Dt = Nu/ P where Nu is the total number of streams and P	Horton, 1932
Aerial	Hypsometric integral (HI)	HI = (ELmean- ELmin) / (ELmax- ELmin)where ELmean is the mean elevation, ELmin is the minimum, and ELmax the maximum elevation	Strahler, 1952
	Bifurcation ratio (Br)	Br = Lu/ Lu+1 where Lu is the number of specified streams and a number of next higher-order streams in basin.	Strahler, 1964
	Asymmetry factor (AF)	AF= Ar/ A where Ar is the area of right side of the basin and A is the total area of basin.	Cox *et. al.,* 1994
	Valley floor width to height ratio (Vf)	Vf= 2Vfw/ (Eld-Esc) + (Erd-Esc), where Vfw= width of valley floor, Eld and Erd= Elevation of left and right valley divides, Esc= Elevation of the valley floor	Bull and McFadden, 1977
Relief	Stream length gradient index (SL)	SL = Δh /ΔI×L, where Δh = Difference in elevation of the ends of the reach, ΔI = Length of reach, L = distance from the midpoint of reach to the most distant point up-stream.	Hack (1973)
	Mean stream length (MSL)	MSL = Lu/Nu, Lu = Total length of all streams in a given order, Nu = Number of stream segments of that order.	Strahler (1964)

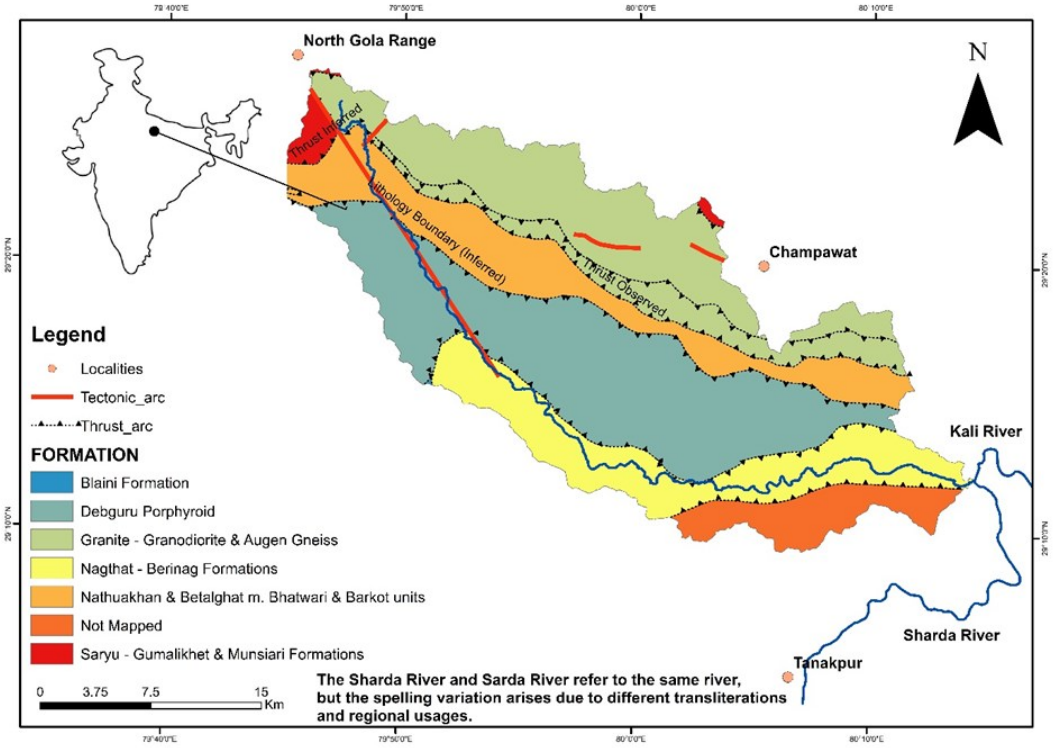

Fig. 1. *Geological and tectonic map of the Ladhiya river basin, displaing spatial arrangement of lithotectonic units, faults, and thrusts*

ther employed to delineate the drainage network and watersheds. Developed by Japan's Ministry of Economy, Trade, and Industry (METI) and launched on NASA's Terra spacecraft in December 1999, ASTER acquires satellite imagery through three specialized telescopes and sensors operating across 14 spectral bands.These include three visible and near-infrared (VNIR) bands with a spatial resolution of 15 meters, six shortwave infrared (SWIR) bands at 30 meters resolution, and five thermal infrared (TIR) bands with a resolution of 90 meters. Each ASTER scene covers a 60×60 km area. Additionally, Band 3 of VNIR provides along-track stereo coverage through a backward-looking telescope, enabling the creation of a high-quality digital elevation model.

Topographic maps at a 1:2,500,000 scale were acquired from the Army Map Services, which publishes them on behalf of the University of Texas at Austin, the responsible organization for their distribution. These maps were georeferenced to the WGS84 datum and

projected using the UTM coordinate system. Using the georeferenced maps, the locations of towns, cities, and villages within the Ladhiya River Basin were vectorized for further analysis.

The primary sources of data on lithology, major tectonic features including thrusts and dislocations as well as smaller faults, joints, and shear zones, were derived from the revised geological map of the Kumaon Himalaya by Valdiya (2010). To ensure consistency with the ASTER DEM and multispectral data used in this study, the map was georeferenced to the WGS84 datum and UTM projection. The ASTER DEM produced by orthographic images. Therefore, it accrues certain errors related to topography, vertical anomalies, and shadowing effects (Han *et al*., 2021). Additionally, geological data were obtained from published geological maps of the Kumaon Himalaya, which were georeferenced as they contained a geographic coordinate system (Fig. 1).

The TauDEM (Terrain Analysis Using Digital Elevation Models) plugin was utilized to generate stream networks and delineate basin boundaries, while also deriving various hydrologic characteristics from the study area's digital elevation data. These hydrologic grids were integrated into the GIS domain to define watershed boundaries and identify all locations within the DEM that are upstream of the specified outlet point (Farooq *et al*., 2015; Khan *et al*., 2023; Khan and Govil, 2023; Khan *et al*., 2024).

Index of relative active tectonic activity

In this study, relative tectonic activity was assessed using geomorphic indices, which were categorized into three levels: low, moderate, and high tectonic activity (Table 1). These classifications were then integrated to develop the Index of Relative Active Tectonic Activity (IRAT). Basins were ranked based on individual geomorphic indices, such as the Hypsometric Integral, where low tectonic activity was assigned rank 1, moderate rank 2, and high rank 3. The final tectonic rank for each basin was determined by averaging these individual rankings.

RESULTS AND DISCUSSION

The Ladhiya River Basin covers an area of 739.45 km^2 and is divided into seven sub-watersheds to derive the different thematic layers. Derived results, the morphotectonic indices were grouped into three sections relief, linear, and aerial parameters.

Stream order (Nu)

Stream ordering refers to the hierarchical classification of streams within a drainage basin. As per Strahler (1952), the ordering process starts from the smallest fingertip tributaries, which have no upstream feeders (drainage network, Fig. 2). The total number of streams (N) for each order (U) in the Ladhiya River Basin is presented in Table 2. The analysis of stream characteristics aligns with Horton's (1945) first law of stream numbering, which suggests that the number of streams in successive orders within a drainage basin follows an inverse geometric ratio (Table 2).

Stream length (Lu)

The total length of streams of a specific order within a basin is a key characteristic. The stream length patterns in the sub-basins align with Horton's (1945) second law, known as the "Law of Stream Lengths." This law states that the average length of streams of each order in a drainage basin tends to closely follow a direct geometric progression. The stream lengths for all sub-basins of different orders were measured using ASTER DEMs. The total stream length of the Ladhiya River Basin is

Table 2. Showing relationship between the total number of streams of each order from top to bottom for each sub-watershed (7 sub-watershed) in first column (F)and the second column displays the total length of each order in the sub-basin

Dholigaon		Bigrakot		Khatoli		Padunga		Baman Jaol		Kukrauni		Sugroan Gaon	
F	L	F	L	F	L	F	L	F	L	F	L	F	L
519	165	452	136	498	148	567	154	209	56	276	72	130	36
253	86	213	67	214	71	269	92	88	31	129	38	64	22
138	46	104	33	124	35	142	47	55	17	54	18	20	13
60	19	65	23	45	13	80	26	18	6	57	18	4	2
67	16	32	11	1	0	39	13	0	0	28	9	0	0
0	0	37	14	117	28	36	11	2	1	7	2	1	0
0	150	0	125	0	134	0	159	13	58	0	75	11	37

F represents the number of streams; L denotes the length in kilometers; stream length values were rounded to whole numbers using standard mathematical rounding. Values greater than 0.5 were rounded up, while values less than or equal to 0.5 were rounded down

1625.21km, with the stream lengths for each order detailed in Table 2.

Drainage density (Dd)

Drainage density is a key morphometric parameter that represents the ratio of the total stream length of all orders within a basin to its area (Horton, 1932). It serves as a quantitative measure to analyze basin evolution and characterizes the drainage fabric by assessing the density of stream channels. Low drainage density is typically found in regions with high permeability, dense vegetation, and gentle topography, whereas high drainage density is associated with rugged, steeply elevated terrains. Additionally, the drainage density of a basin is shaped by geological and climatic conditions and is determined using the following equation.

$$Dd = \frac{Lu}{A}$$

Here, Lu represents the total length of streams of all orders within a basin, while A denotes the basin area. The drainage density for each of the 18 sub-basins was calculated and categorized into three classes to analyze the results. Several faults and thrusts have been identified within the Ramganga River Basin (see Geological Map), highlighting the region's substantial tectonic influence. Tectonic activity plays a major role in driving erosion and upliftment. The findings indicate that the central-western region exhibits a high drainage density, suggesting stronger tectonic influence relative to erosion, whereas the northern and south-central regions display lower drainage density (Fig. 2).

Drainage texture (T)

Drainage texture is defined as the ratio of the total number of stream segments of all orders to the perimeter of the basin (Horton, 1945). It has been observed that the drainage texture is directly influenced by the basin's infiltration capacity basin's perimeter and is governed by various natural factors, including climate, rainfall, vegetation cover, rock and soil composition, relief, and basin evolution (Smith, 1950; Khan *et al*., 2024). The following equation is used to compute drainage texture.

$$T = \frac{Nu}{P}$$

Drainage texture (T) is determined using the basin perimeter (P) and the total number of stream segments across all orders (Nu). The computed results for 7 sub-basins were categorized into three classes. Fine drainage texture was identified in the northern extremity) and central-eastern border, whereas the northern and southern sub-basins exhibited a moderate texture. In contrast, the central sub-basins displayed a low drainage texture. The southern extremity expresses low drainage texture, exhibits old and eroded landscape (Fig. 3).

Hypsometric integral (HI)

The HI is a dimensionless parameter that allows for a scale-independent comparison of various watersheds or catchments. It serves as an indicator of landscape evolution, where low HI values signify highly eroded terrains (late stage), moderate values represent mature

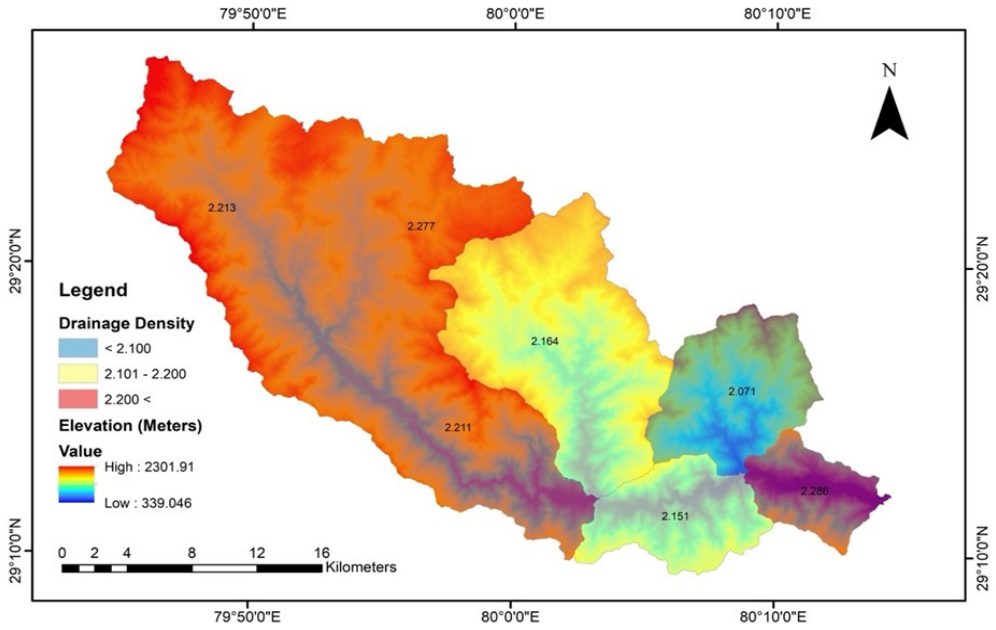

Fig. 2. *Exhibiting drainage density and its spatial variation in the Ladhiya river basin*

landscapes, and high values correspond to youthful landscapes. The hypsometric integral is calculated using the following formula.

$$HI = \frac{Elmean - Elmin}{(Elmax - Elmin)}$$

Elmin represents the basin's minimum elevation, Elmax denotes its maximum elevation, and Elmean refers to the mean elevation. The hypsometric integral (HI) values range from 0 to 1. Earlier, computational limitations made HI calculations complex and resource-intensive. However, the advent of digital elevation models (DEMs) has significantly improved the accuracy and efficiency of detecting active tectonics worldwide (Dowling *et al*., 1998; Khan and Govil, 2023; Khan *et al*., 2024).

The Ladhiya River Basin, situated in the Outer Lesser Kumaon Himalaya, has an elevation range between 371 meters and 2261 meters, indicating a steep gradient. The results from 7 sub-basins reveal HI values ranging from 0.33 to 0.54, corresponding to low to high tectonic activity. The Dholigaon, Bigrakot, Padunga, and Kukraini sub-basins, located within the main valley and aligned to the left flank of the trunk stream, exhibit high HI values, indicating a high rate of uplift and active tectonics potential. In contrast, Khatauli and Baman Jaol, situated on the river's right bank and composing trunk stream, display more erosive forces and moderate tectonic influence. Similarly, significant tectonic activity is observed in the south-eastern sub-basin (Sugroan village) while the remaining sub-basins exhibit moderate tectonic influence due to the presence of both known and unidentified faults and thrusts (Fig. 4).

Bifurcation ratio (Rb)

The Rb is defined as the number of streams of a given order divided by the number of streams of the next higher order (Schumm, 1956). According to Horton (1945), it serves as an index that reflects a basin's relief and degree of dissection. While Rb typically exhibits minimal variation under different environmental conditions, notable deviations occur in regions where geological factors dominate. The calculation is performed using the following equation.

$$Rb = \frac{\sum nu}{\sum Nu + 1th\ order}$$

Here, Nu represents the total number of streams of a given order, while Nu+1 denotes the total number of streams of the next higher order. Lower bifurcation ratio (Rb) values are associated with gently rolling terrain and low-elevation watersheds, whereas higher values indicate strong tectonic influence on basin evolution. Additionally, Eze and Effong (2010) observed that elevated Rb values suggest a lower risk of flash floods within the basin.

The bifurcation ratio varies widely in the Ladhiya river basin, with values ranging from 0.56 to 12.94 (Fig. 5). It indicates that tectonic and erosive forces in the basin are strongly interacting. Because of the strong elevation gradient that creates a substantial path for water to flow, most sub-basins from north to south have low bifurcation ratio values along the right flank of the river, which causes more erosion, resulting higher rate of uplift and tectonics. However, it was also noted that more erosion occurs when different tectonic features strike with each other.

Asymmetry factor

The asymmetry factor (AF) is a significant morphotectonic parameter used to detect tectonic tilting within a drainage basin (Cox *et al*., 1994; Keller and Pinter, 2002; El Hamdouni *et al*., 2008; Khan *et al*., 2024). It operates on the assumption that a river flowing through a homogeneous lithological terrain, minimally influenced by erosion and tectonic activity, should exhibit a symmetric drainage pattern. The AF is defined as.

$$AF = 100\left(\frac{Ar}{At}\right)$$

Where Ar is the right-side area of the basin from the trunk stream (headwater to outlet) and At is total area of the basin.

The asymmetry factor (AF) values for the seven sub-basins of the Ladhiya River range from 45 to 56 (Fig. 6). To assess tectonic significance, these values were categorized into three classes based on basin tilting. Sub-basins classified as nearly symmetric received a low rank, while those with high asymmetry were ranked higher. Increased tilting and asymmetry are observed in tectonically active regions, where intensified erosion influences basin evolution. At a regional scale, tectonic activity is indicated by the tilting and migration of higher -order streams, whereas localized tectonic activity is reflected in increased sub-basin asymmetry (Keller and Pinter, 2002). The Ladhiya River basin exhibits significant asymmetry on both banks, with notably low asymmetry in the northeastern and extreme southern sub-basins. Lower AF values in the central and south-central sub-basins suggest that tectonic forces have shifted the trunk stream to the right. Observations indicate that the Ladhiya River's main channel continues to migrate due to persistent tectonic influences, evident in existing faults and thrusts (Fig. 6).

Valley floor width to height ratio

Bull and McFadden (1977) used the valley floor width-to-height ratio to identify active tectonics and differentiate open from broad valleys. Tectonically active regions exhibit pronounced valley morphology variations, ranging from V-shaped to U-shaped profiles, reflecting a state of dynamic geomorphic equilibrium.. Silva *et al*. (2003) explored the distinctions between broad-floored,

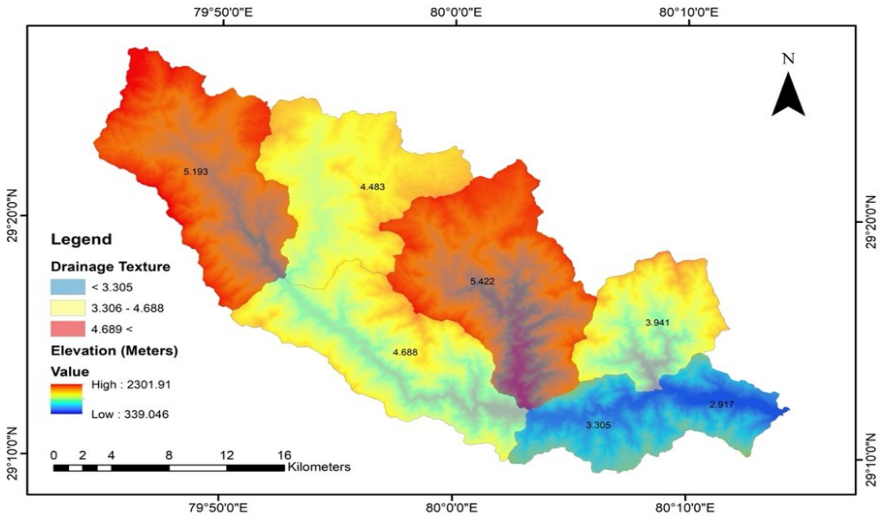

Fig.3. *Showing the spatial variation of the drainage network spacing across the basin*

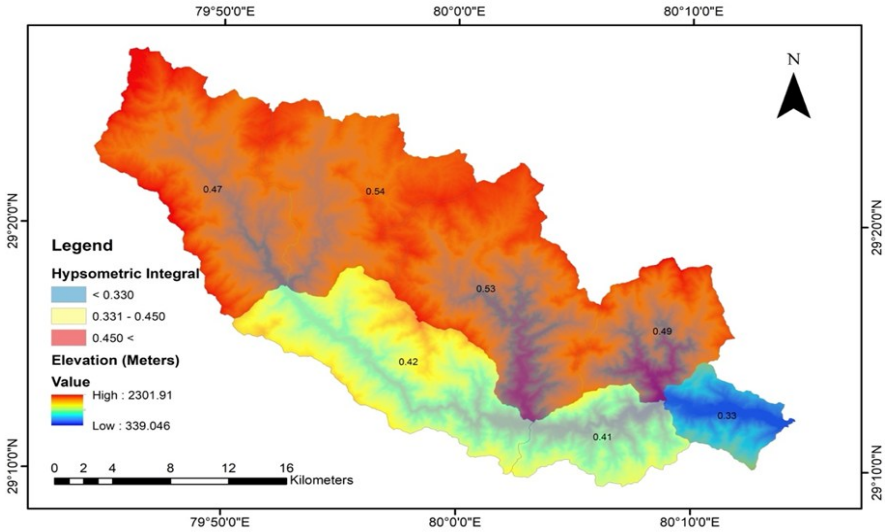

Fig. 4. *Displaying the spatial arrangement of Hypsometric Integral to determine the youthfulness of the basi.*

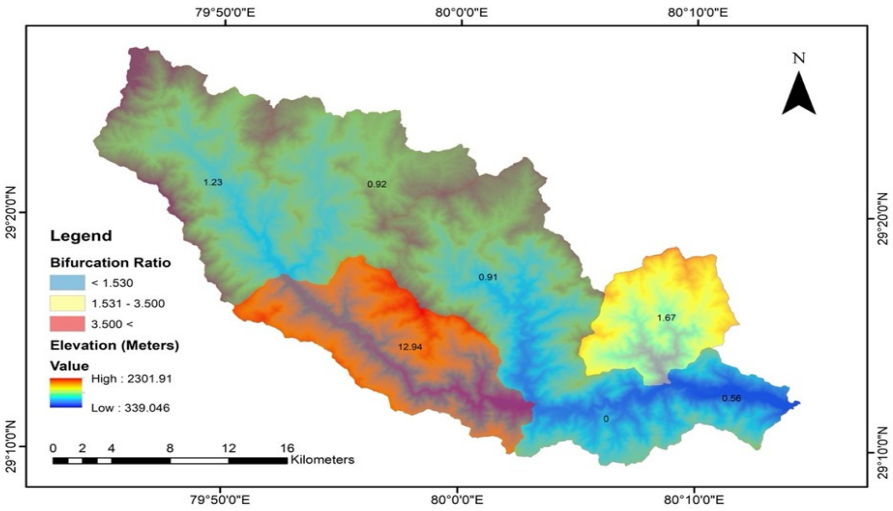

Fig. 5. *Showing the bifurcation ratio and its distribution across the basin*

U-shaped valleys with primarily lateral erosion into nearby hills in response to tectonic quiescence, and V-shaped valleys occupied by streams incising their bedrocks in response to active uplift. The Vf index is calculated by the equation.

$$Vf = \frac{2Vfw}{(Eld - Esc) + (Erd - Esc)}$$

Where Vf is the ratio of the valley floor width to the height, Vfw is the valley width, Eld is the left divide's elevation, Esc is the valley floor's elevation, and Erd is the right divide's elevation (Fig. 7).

The Ladhiya River flows west to east before merging with the Kali River. As it travels from the Gola Range to Surgoan Village, it traverses diverse lithological and structural domains, which significantly influence its transformation from steep V-shaped valleys to moderately uplifted U-shaped valleys. The findings on the valley floor width-to-height ratio (Vf) suggest that the Ladhiya River basin is primarily influenced by structural controls, while the sub-basins along the mainstream show more pronounced erosive effects. Vf values range from 0.29 to 0.74, highlighting a continuous interaction between erosional and tectonic forces. Sub-basins aligned perpendicular to the trunk stream display pronounced tectonic influence, whereas the trunk stream shapes sub-basins differently, favoring rapid erosion in areas with lower uplift rates (Fig. 7).

Stream length gradient

The stream length gradient serves as a key indicator of erosion intensity, illustrating how soil and rock are sculpted and reshaped across a river basin (Hack, 1973). In neo-tectonically active terrain, the rate of erosion determines the rate of uplift, which results in a longitudinal profile that is slightly concave (Schumm *et al*., 2002), and leads to crustal stability. However, tectonic, lithological, and climatic variables impact the stability of the terrain. Stream length gradient is defined as

$$SL = \frac{\Delta H}{\Delta L}$$

Where ΔH is the change in the elevation for a selected reach, and ΔL is the length of the reach and L is the total planimetric length from the midpoint of the reach to the highest point on the channel (Mahmood and Gloaguen, 2012; Khan *et al*., 2024). Further, the stream length gradient was computed for 7 sub-basins of the Ladhiya river basin. The findings indicate that the northwest sector of the basin is markedly shaped by tectonic forces, while the sub-basins intersecting the main channel display comparatively subdued tectonic activity. However, low values also correspond to the tectonic activity due to transecting faults and thrusts across the basin (Fig. 8).

Mean stream length (MSL)

This index is essential for analyzing and interpreting the morphometric and hydrological characteristics of a basin. It represents the average length of streams of a particular order within a drainage basin and is a fundamental aspect of Horton's laws of drainage composition (Horton, 1945; Strahler, 1957; Schumm, 1956; Chorley *et al*., 1984; Keller and Pinter, 2002). The Mean Stream Length (MSL) offers valuable insights into the geometric and hierarchical arrangement of stream networks, highlighting the basin's geomorphological evolution, erosion dynamics, and hydrological patterns. The mean stream length ratio was determined by first calculating

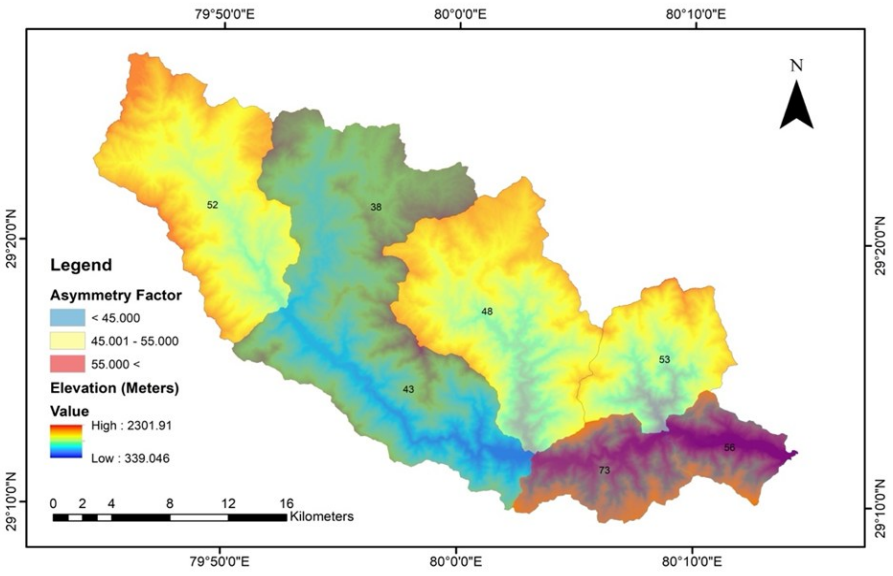

Fig. 6. *Displaying the asymmetry factor, and exhibits its spatial arrangement*

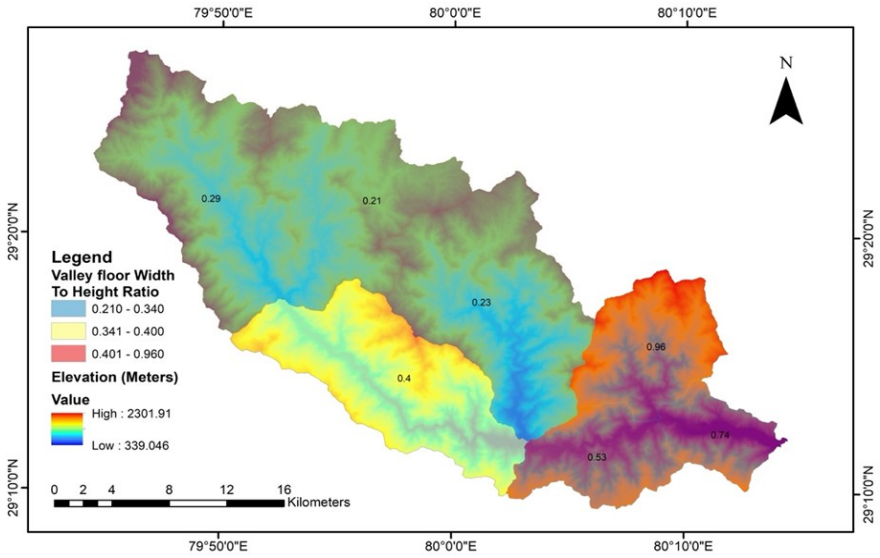

Fig. 7. *Valley floor width to height ratio exhibiting spatial arrangement of river basin to understand the active tectonics.*

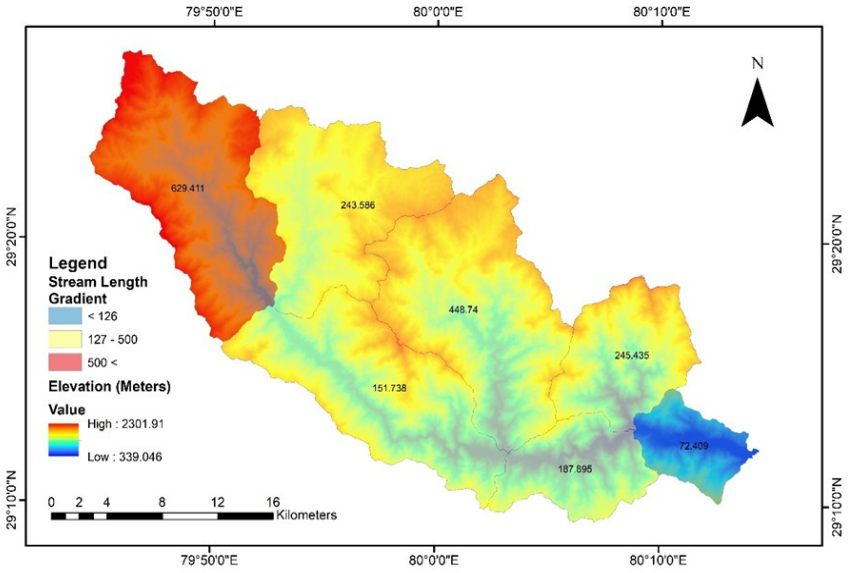

Fig. 8. *Stream length gradient showing power of erodibility of the basin*

the stream length ratio for different stream orders within the basin. It was then computed using the following formula.

$$Lsm = \frac{Lu}{nu}$$

Where Lu is the mean length of all streams of one order and nu is the total number of streams of lower order. The values range between 0.21 and 0.30 across the sub-basins. The values were calculated for each sub-basin and each order and in the end, the averaged out to provide a representative value for each sub-basin.

It was observed that low MSL values typically indicate high drainage density, unstable processes, and high erosion rates while high MSL values suggest low drainage density, relatively stable processes, and efficient sediment transport. These variations provide significant insights for effective basin management, flood risk assessment, and water resource planning. Further, these values have been classified into three classes displaying low, moderate, and high values, corresponding to active tectonics (Fig. 9).

River profile

River profiles, particularly longitudinal profiles, are valuable geomorphic indicators that provide insights into the interplay between fluvial processes and tectonic activity

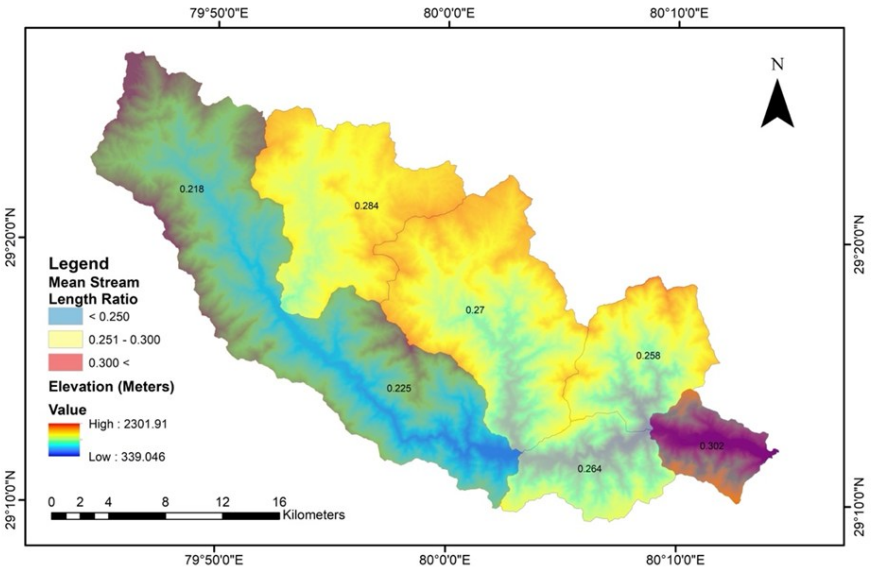

Fig.9. *Mean stream length shows its spatial fabric, providing insights about tectonic influence*

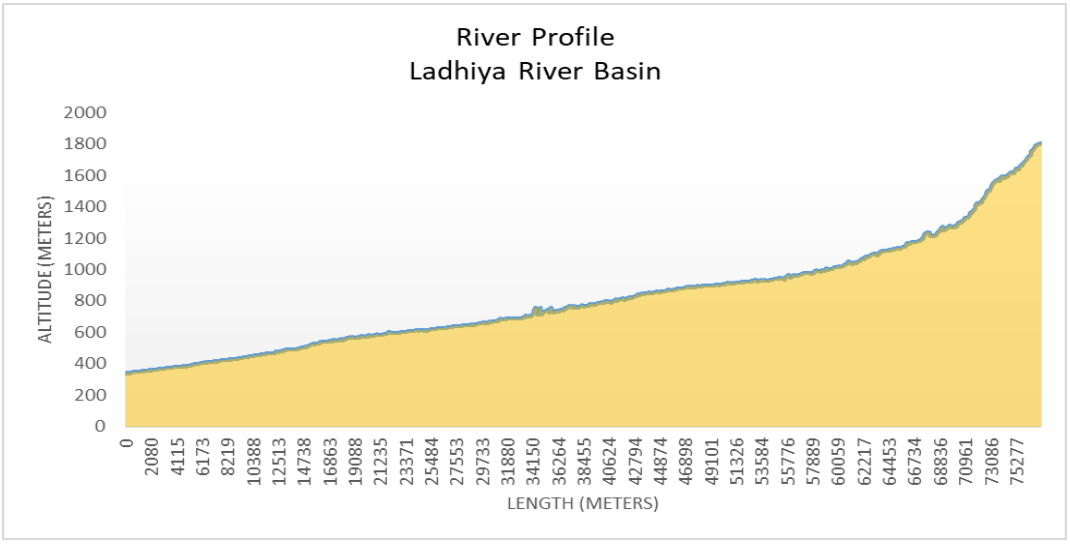

Fig. 10. *Ladhiya River profile showing a concave structure, demonstrating multiple knick points and tectonic control. The X-axis shows the length of river while Y-axis displays elevation from outlet to headwater.*

The shape and gradient of a river profile are influenced by factors such as lithology, climate, and tectonic uplift (Fig. 10). In regions with active tectonics, river profiles often exhibit distinct anomalies, such as knick points, steep gradients, and changes in channel morphology, which can be used to infer tectonic activity. A river's longitudinal profile is a plot of elevation against distance along the river channel. In tectonically active regions, these profiles often deviate from the typical concave-upward shape due to uplift or faulting (Fig. 11).

Field and other evidence of active tectonics

In addition to morphotectonic indices, ongoing deformation can be evaluated through the type, scale, magnitude, and timing of landscape and landform features it generates. Geomorphic features serve as key indicators of active tectonics. Several neotectonic landforms encompass fault gouge and breccia outcrops, hydrothermally altered mineral assemblages along fault zones, fault scarps, landslides, unpaired river terraces, river ponding, paleochannels, paleolake deposits, uplifted potholes, deep gorges with convex walls, and laterally displaced streams. (e.g., Valdiya, 2001; Schumm *et al*., 2002; Thakur, 2004; Kothyari and Pant, 2008; Khan *et al*., 2024). Drainage networks in tectonically active regions are highly responsive to tectonic forces and erosional processes, making them valuable indicators for deciphering the tectonic characteristics of a given area (e.g., Beneduce *et al*., 2004; Bull, 2007; Bishop *et al*., 2005; Ribolini and Spagnolo, 2008; Pérez-Peña *et*

Fig. 11. *Knick point profile A showing that the Ramgarh Thrust and many faults run along the river, indicative of current neotectonic control. The altitude is show at X -axis and length at Y-axis (Unit of measurement is meter).*

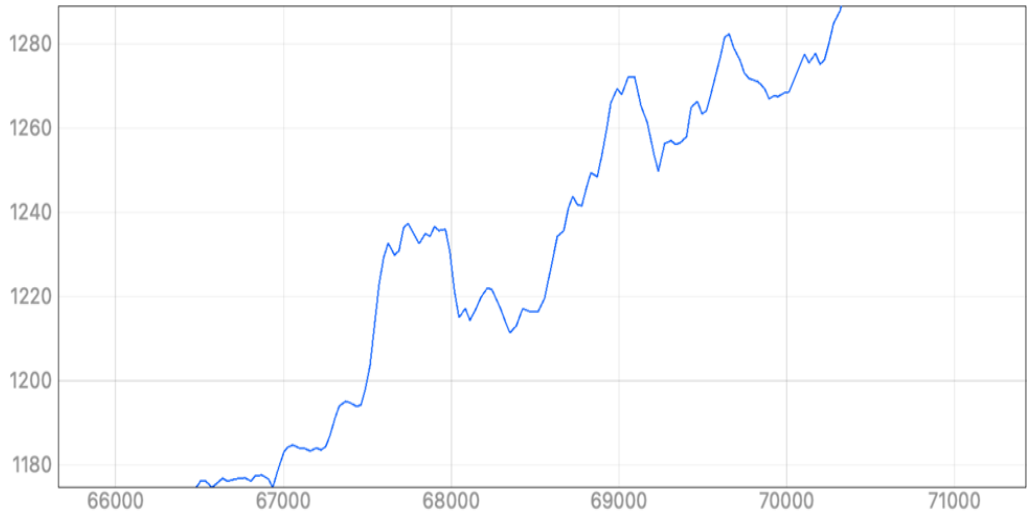

Fig.12 . *The Ladhiya river exhibiting many knick points near to the headwater due to faulting; Geo-tectonic map displays inferred faults run across the river; the altitude shown at X -axis and length at Y-axis (Unit of measurement is meter)*

al., 2010; Mumipour and Nejad, 2011; Parveen, 2020; Hassan *et al*., 2024).

The field evidence of tectonic influence along the Ladhiya River Basin (Fig. 12 and 13) was collected and coupled with satellite imageries (Google Earth Pro) to delineate nick points, fault scarps, straight and meandered river courses, abrupt changes in flow direction, fault gouges, etc.

Index of relative active tectonics

Relying on a single index to assess active tectonics may lead to ambiguous or conflicting results. A more precise evaluation of a region's tectonic activity is achieved through the integration of multiple indices (Dowling *et al*., 1998; Ali and Iqbal, 2020; Khan *et al*., 2024). This study examined active tectonics within a moderately sized area (739 km²), divided into seven sub-basins, using eight morphotectonic indices. Each sub-basin was ranked on a scale of 1 to 3 based on individual index values. A basin experiencing the highest tectonic activity would score 27, while the least active would score 9. A final Index of Relative Active Tectonics (IRAT) map was generated based on these rankings to visualize the spatial distribution of tectonic activity.

The main trunk stream of the Ladhiya River flows over 77 kilometers before merging with the Kali River at Chuka Gaon. To assess the tectonic activity, nine morphotectonic indices were calculated, categorizing the basin into zones of low, moderate, and high tectonic activity. These indices were aggregated to derive the final Index of Relative Active Tectonics (IRAT) ranking for each sub-basin. The geological map (Fig. 1) highlights that the river basin intersects several major thrusts, including the South Almora Thrust (SAT) and the Main Boundary Thrust (MBT) in the south, as well as the Ramgarh Thrust (RT), which runs parallel to the main trunk stream.

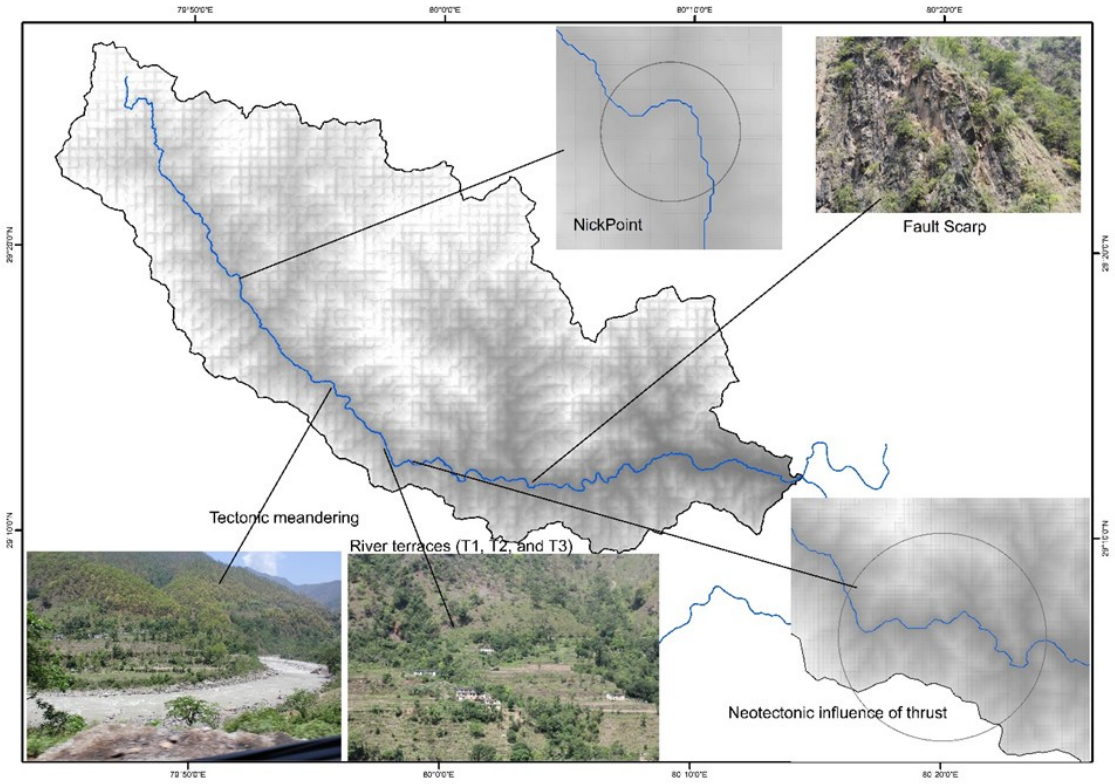

Fig. 13. *Ladhiya river basin exposing numerous additional pieces of evidence of active tectonics viz., fault scarps, knick points, tectonically*

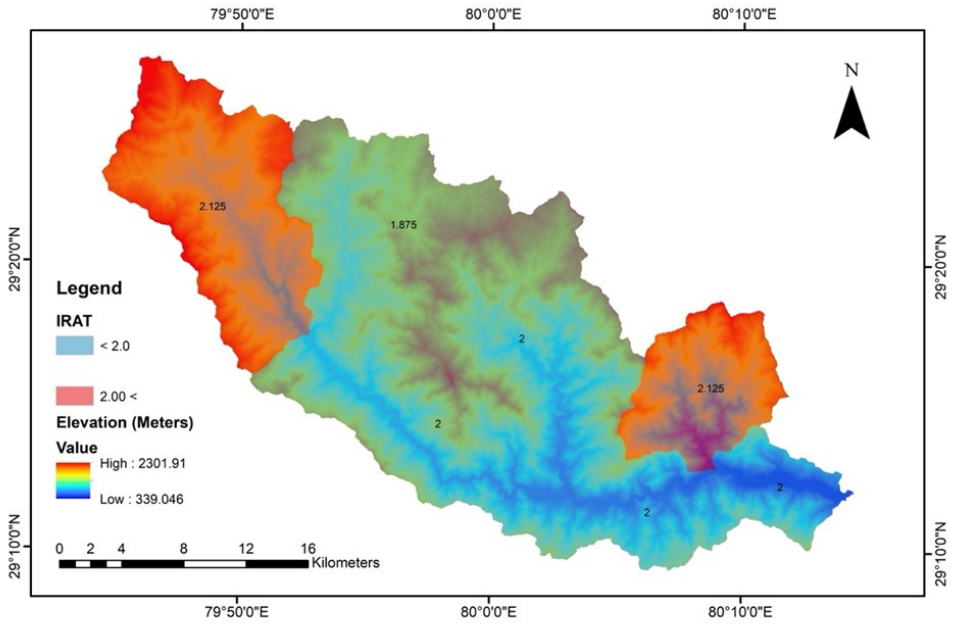

Fig. 14. *Displaying the index of relative active tectonics (IRAT)*

Active faults are recognized as primary sources of earthquakes of varying magnitudes in seismically active regions worldwide. Their identification is crucial for understanding the active tectonics of such zones, particularly in the Himalayan region, one of the most seismically active intercontinental areas globally. The ongoing crustal deformation in this region is evident from the occurrence of small-, medium-, and large-magnitude earthquakes along the Himalayan arc. Notable large-magnitude earthquakes in the past century include the 1897 Shillong (M 8.7), 1905 Kangra (M 8.6), 1934 Bihar (M 8.7), and 1950 Upper Assam (M 8.5) earthquakes (Seeber and Armbruster, 1981; Yeats *et al*., 1997; Malik and Nakata, 2003). The Main Central

Thrust (MCT) and Main Boundary Thrust (MBT) are identified as key zones of Cenozoic shortening across the Himalayas (Gansser, 1964; Valdiya *et al*., 1984). However, the current tectonically active boundary between the Indian and Eurasian plates is marked by the Himalayan Frontal Fault (HFF) (Nakata, 1989). The Ladhiya River Basin, situated between the South Almora Thrust and the Main Boundary Thrust, is significantly influenced by these tectonically active structures, which play a dominant role in the basin's evolution. The morphotectonic parameters individually and collectively indicate strong tectonic influence over the river.

The northern part of the drainage basin is heavily influenced by tectonic forces, primarily due to intense tectonic activity along the Ramgarh Thrust (RT). In the Northern Central and South Central sub-basins, there is a noticeable interplay between tectonic forces and erosional processes. This dynamic interaction is supported by geomorphic indices such as drainage density, drainage texture, bifurcation ratio, and stream length gradient, which collectively highlight the ongoing struggle between tectonic uplift and erosion (Fig. 14).

Basin asymmetry further reveals that the trunk stream shifts both southward and northward, creating meanders in several areas within the Central region. This meandering pattern, along with other tectonic indicators, underscores the significant tectonic control shaping the basin's morphology.

Conclusion

This study underscores the importance of integrating multiple morphotectonic indices to accurately assess active tectonics, as relying on a single index can lead to ambiguous or conflicting results. Therefore, the present study examined nine morphotectonic indices across seven sub-basins within the Ladhiya River Basin, Eastern Kumaun Himalaya, based on a detailed assessment of the region's tectonic activity. The derived results of each indicator displayed a remarkable fact that river basisn is under constant evolution in the form of struggle between erosive forces and tectonic uplift. For example, western extremity and sub-basin on the south - south north indicated strong tectonic influence, clearly revealing in the final results of the Index of Relative Active Tectonics (IRAT). Further, the results emphasized the dominant role of tectonic forces, especially along the Ramgarh Thrust (RT), South Almora Thrust (SAT), and Main Boundary Thrust (MBT), in shaping the basin's evolution while the sub-basin on the right bank shows high impact of erosive forces. It was also concluded that the southward movement of tectonic forces may cause disturbances in the river basins aligned from west to east, indicating the need for careful consideration before constructing mega structures in the close vicinity of river channels.The interplay between tectonic uplift and erosional processes is evident in the Northern Central and South Central sub-basins, supported by geomorphic indices such as drainage density, drainage texture, bifurcation ratio, and stream length gradient. Additionally, basin asymmetry and meandering patterns of the trunk stream further emphasize the strong tectonic control shaping the basin's morphology. Situated in the seismically active Himalayan region, the Ladhiya River Basin exemplifies the dynamic tectonic processes driven by the ongoing collision between the Indian and Eurasian plates.

Conflict of interest

The authors declare that they have no conflict of interest.

Author contributions

Mohd Nazish Khan: Conceptualization, supervision, methodology, writing – review & editing, project administration, and funding acquisition. M. Suhail: Investigation, data collection, and resources. Dilawez Ali: Conceptualization, writing – original draft, software, formal analysis, methodology, data curation, validation, and visualization. Mohammad Faizan: Investigation, data processing, and validation. Samyayev Anvar Kadirovich: resources, technical support, and review. Egamberdiev Asamberdi: Visualization support, data assistance.

REFERENCES

1. Agarwal, P. K., Bain, P. M. & Chamberlain, R. W. (2012). The value of applied research: Retrieval practice improves classroom learning and recommendations from a teacher, a principal, and a scientist. *Educational Psychology Review*, 24(3), 437–448. https://doi.org/10.1007/s10648-012-9210-2.
2. Ahmad, T., Harris, N., Bickle, M., Chapman, H., Bunbury, J. & Prince, C. (2000). Isotopic constraints on the structural relationships between the lesser Himalayan series and the high Himalayan crystalline series, Garhwal Himalaya. *Geological Society of America Bulletin*, 112(3), 467-477. https://doi.org/10.1130/0016-7606(2000)112
3. Ali, S.A. & Iqbal, J. (2020). Assessment of relative active tectonics in parts of Aravalli mountain range, India: implication of geomorphic indices, remote sensing, and GIS. *Arabian Journal of Geoscience,* 13, 57. https://doi.org/10.1007/s12517-019-5028-24.
4. Arisco G, Arnone G & Favara R, *et al*. (2006) Integrated neotectonic and morphometric analysis of northern Sicily. *Bollettino della Società Geologica Italiana,* 125, 1-24.
5. Beaumont, C. R., Jamieson, A., M.H. Nguyen & Lee B. (2001). Himalayan tectonics explained by extrusion of alow-viscosity crustal channel coupled to focused surfacedenudation, *Nature*, 414, 738-742. https://doi.org/10.1038/414738a8.
6. Beneduce, P., Festa, V., Francioso, R., Schiattarella, M.

& Tropeano, M. (2004). Conflicting drainage patterns in the Matera Horst Area, southern Italy. *Physics and Chemistry of the Earth*, 29(10), 717-724. https://doi.org/10.1016/j.pce.2004.03.002
7. Bishop, M.P., Shroder, J.F., Jeffrey, Jr. & Colby, D. (2003). Remote sensing and geomorphometry for studying relief production in high mountains. *Geomorphology*, 55, 345-361.3. https://doi.org/10.1016/S0169-555X(03)00149-1
8. Bull, W.B. (2007). Tectonic geomorphology of mountains: A new approach to paleoseismology. Wiley-Blackwell, Oxford, 328.
9. Bull, W.B. & McFadden, L. (1977). Tectonic geomorphology north and south of the garlock fault, California. In D. O. Dohering (Ed.), Geomorphology in arid regions (115–128). *Geomorphology, State University of New York*.
10. Burtman, V. S. & Molnar, P. (1993). Geological and geophysical evidence for deep subduction of continental crust beneath the Pamir (Geological Society of America Special Paper 281). *Geological Society of America*, https://doi.org/10.1130/SPE281-p1.
11. Chorley, R. J., Schumm, S. & Sugden, D. E. (1984). Geomorphology . *Methuen and Co.*
12. Cox, R. T. (1994). Analysis of drainage basin symmetry as a rapid technique to identify areas of possible Quaternary tilt-block tectonics: An example from the Mississippi Embayment. *Geological Society of America Bulletin*, 106 (5), 571–581.
13. DeCelles, P. G., Gehrels, G. E., Quade, J., LaReau, B. & Spurlin, M. (2000). Tectonic implications of U-Pb zircon ages of the Himalayan orogenic belt in Nepal. *Science*, 288(5465), 497-499. https://doi.org/10.1126/science.288.5465.497
14. DeCelles, P.G., Robinson, D.M., Quade, Ojha, J., T.P. Garizone, C.N. Copeland, P. & Upreti, B.N. (2001). Stratigraphy, structure, and tectonic evolution of the Himalayan fold-thrust belt in western Nepal. *Tectonics*, 20, 487–509. https://doi.org/10.1029/2000TC00122612.
15. Dewey, J.F. & Bird, J.M. (1970). Mountain belts and the new global tectonics. *J. Geophys. Res.,* 75, 2625-2647. https://doi.org/10.1029/JB075i014p0262513.
16. Dowling, T.I., Richardson, D.P., O'Sullivan, A. Summerell, G.K. & Walker, J. (1998). Applications of the hypsometric integral and other terrain based metrices as indicators of catchment health: A preliminary analysis. CSIRO Land and Water, (Canberra). *Technical Report,* 20/98, 49.
17. El Hamdouni, R. Irigaray, C. Fernández, T. Chacón, J. & Keller, E. A. (2008). Assessment of relative active tectonics, southwest border of the Sierra Nevada (southernSpain), *Geomorphology*, 96, 150–173. https://doi.org/10.1016/j.geomorph.2007.08.00415.
18. Eze, B. E. & Effiong, J. (2010). Morphometric parametersof the Calabar River Basin: Implication for hydrologic pro-cesses. *Journal of Geography and Geology*, 2, 18-26. https://doi.org/10.5539/jgg.v2n1p1816
19. Farooq, S., Khan, M. N. & Sharma, I. (2015). Assessment of active tectonics in Eastern Kumaon himalaya on the basis of morphometric parameters of goriganga river basin, *IJAEES*, 3(3), 14-21.
20. Gansser, A. (1964). Geology of the Himalayas. *Wiley InterScience, New York*, 289.
21. Hack, J. T. (1973). Stream-profile analysis and stream-gradient index. *United States Geological Survey Journal of Research*, 1(4), 421–429.
22. Hallet, B. & Molnar, P. (2001). Distorted drainage basins as markers of crustal strain east of the Himalaya. *Journal of Geophysical Research: Solid Earth*, 106 (B7), 13697-13709. https://doi.org/10.1029/2000JB900335
23. Han, H., Zeng, Q. & Jiao, J. (2021). Quality assessment of TanDEM-X DEMs, SRTM and ASTER GDEM on selected chinese sites. *Remote Sensing*, 13(7), 1304. https://doi.org/10.3390/rs13071304.
24. Harrison, T. M., Copeland, P., Kidd, W. S. F. & Yin, A. N. (1992). Raising tibet. *Science*, 255 (5052), 1663-1670. https://doi.org/10.1126/science.255.5052.1663
25. Hassan, T., Hadji, R., Hamed, Y., Gentilucci, M. & Badri, K. (2024). Integrated geospatial analysis for identifying regions of active tectonics in the Saharian Atlas: A review analysis of methodology and calculation fundamentals. *Journal of African Earth Sciences,* 211, 105188. https://doi.org/10.1016/j.jafrearsci.2024.105188
26. Horton, R. E. (1932). Drainage basin characteristics. *Trans. Am. Geophys. Union*, 13, 350-361.
27. Horton, R. E. (1945). Erosional development of streams and their drainage basins: Hydrophysical approach to quantitative morphology. *Geological Society of America Bulletin*, 56(3), 275-370.
28. Husson, L., Bernet, M., Guillot, S., Huyghe, P., Mugnier, J. L., Replumaz, A., Robert, X. & Van der Beek, P. (2014). Dynamic ups and downs of the Himalaya Geology, *Geological Society of America,* 42(10), 839–842. https://doi.org/10.1130/G36077.1
29. Kalpana, G., Kothyari, G. C. & Kotlia, B.S. (2023). Morphotectonic assessment of the Gaula river basin, Kumaun lesser Himalaya, Uttarakhand. *Quaternary Science Advances*, 12, 100- 115. https://doi.org/10.1016/j.qsa.2023.100115.24.
30. Keller, E. A. & Pinter, N. (2002). Active tectonics: Earthquakes, Uplift, and Landscape. *Prentice Hall*.
31. Khan, M. N. & Govil, H. (2023). Assessment of On-going tectonic deformation in the Goriganga River Basin, Eastern Kumaon Himalaya using geospatial technology. *Journal of Applied and Natural Science*, 15(4), 1679 – 1690. https://doi.org/10.31018/jans.v15i4.5042
32. Khan, M.N., Suhail, M., Dilawez, A., Jafri, S. M. W. H. & Jamshid, J. (2024). Neotectonic appraisal of Ramganga River basin, Eastern Kumaun, Himalaya, India. *Journal ofApplied and Natural Science*, 16(4), 1690 - 1701. https://doi.org/10.31018/jans.v16i4.5928
33. Koons, P.O. (1995). Modelling the topographic evolution of collisional belts. *Annual Reviews Earth and Planetary Sciences* 23, 375-408. https://doi.org/10.1146/annurev.ea.23.050195.002111
34. Kothyari G.C. & Pant P.D. (2008). Evidence of activede formation in the Northwestern part of Almora in Kumaon-Lesser Himalaya: A geomorphic perspective. *Jour. Geol.Soc. Ind.,* 72, 353-364.29. https://doi.org/10.1007/s12594-008-0092-5
35. Kothyari, G. C. Kotlia, B. S., Talukdar, R., Pant, C. C. &Joshi, M. (2020). Evidences of neotectonic activity along Goriganga River, Higher Central Kumaun Himalaya, India. *Geological Journal*, 55 (9), 0072- 1050. https://doi.org/10.1002/gj.379132.

36. Kothyari, G. C., Kandregula, R. S. & Luirei, K. (2017). Morphotectonic records of neotectonic activity in the vicinity of North Almora Thrust Zone, Central Kumaun Himalaya. *Geomorphology*, 285, 272–286. https://doi.org/10.1016/j.geomorph.2017.03.041.
37. Kothyari, G.C. & Luirei, K. (2016). Late Quaternary tectonic landforms and fluvial aggradation in the Saryu River valley: Central Kumaun Himalaya. *Geomorphology*, 268, 159-176. https://doi.org/10.1016/j.geomorph.2016.06.010.34.
38. Kothyari, G.C., Joshi, N., Taloor, A.K., Kandregula, R. S., Kotlia, B.,S. Pant, C.C. & Singh, R. K. (2019). Landscape evolution and deduction of surface deformation in the-Soan Dun, NW Himalaya, India. *Quaternary International*, 507, 302-323. https://doi.org/10.1016/j.quaint.2019.02.016.33.
39. Luirei, K., Longkumer, L., Kothyari, G. C., Rawat, S. & Nain, M. Z. (2022). Tectonic implication in the evolution of lake and Quaternary landforms in the Lohawati river basin, Kumaun outer Lesser Himalaya. *Journal of Asian Earth Sciences*, X, 7, 100102. https://doi.org/10.1016/j.jaesx.2021.100102
40. Mahmood, S. A. & Gloaguen, R. (2012). Appraisal of active tectonics in Hindu Kush: Insights from DEM derived geomorphic indices and drainage analysis. *Geoscience Frontiers*, 3(4), 407-428. https://doi.org/10.1016/j.gsf.2011.12.00235.
41. Malik, J. N. & Nakata, T. (2003). Active faults and related late quaternary deformation along the northwestern Himalayan Frontal Zone, India. *Annals of Geophysics*, 46(5).
42. Marple, R. & Talwani, P. (1993). Evidence of possible tectonic up warming along the South Carolina coastal plain from an examination of River Morphology and Elevation data. *Geology*, 21, 651-654. https://doi.org/10.1130/0091-7613(1993)021
43. McKenzie, D. Sclater, J. G. (1971). The evolution of the Indian Ocean since the late cretaceous. *Geophysical Journal International*. 24 (5), 437. https://doi.org/10.1111/j.1365-246X.1971.tb02190.x
44. Molnar, P. & Tapponnier, P. (1975). Cenozoic tectonics of Asia: Effects of a continental collision, *Science,* 189, 419-426. https://doi.org/10.1126/science.189.4201.419
45. Mumipour, M. & Nejad, H.T. (2011). Tectonic geomorphology setting of Khayiz Anticline derived from GIS processing, Zagros Mountains, Iran. *Asian Journal of Earth Sciences,* 4(3), 171-182. https://doi.org/10.3923/ajes.2011.171.182
46. Nakata, T. (1989). Actives faults of the Himalaya of India and *Nepal. Geological Society of America (Special Paper)*, 232, 243–264.
47. Ouchi, S. (1985). Response of alluvial rivers to slow active tectonic movement. *Geological Society of America Bulletin,* 96, 504-515. https://doi.org/10.1130/0016-7606(1985)96
48. Pant, C.C. & Singh, S.P. (2017). Morphotectonic analysis of Kosi River basin in Kumaun Lesser Himalaya: an evidence of neotectonics. *Arab Journal Geosciences,* 10, 421. https://doi.org/10.1007/s12517-017-3213-8.39
49. Pant, P. D., Chauhan, R. & Bhakuni, S. S. (2012). Development of transverse fault along North Almora Thrust,Kumaun Lesser Himalaya, India: A study based on fieldand magnetic fabrics. *Journal Geological Society of India*, 79, 429–448. https://doi.org/10.1007/s12594-012-0068-140.
50. Parvin, M. (2020). Assessment of active tectonics of the Karrand River Basin using drainage network feature analysis. *Physical Geography Research,* 52(3), 499-514. https://doi.org/10.22059/jphgr.2020.301546.5946
51. Pérez-Peña, J.V., Azor, A., Azanon, J.M. & Keller, E.A. (2010). Active tectonics in the Sierra Nevada (Betic Cordillera, SE Spain): Insights from geomorphic indexes and drainage pattern analysis. *Geomorphology*, 119 (1-2), 74-87. https://doi.org/10.1016/j.geomorph.2010.02.020
52. Ramstein, G., Fluteau, F., Besse, J. & Joussaume, S. (1997). Effect of orogeny, plate motion and land–sea distribution on Eurasian climate change over the past 30 million years. Nature, 386(6627), 788–795. https://doi.org/10.1038/386788a0.
53. Ribolini, A. & Spagnolo, M. (2008). Drainage network geometry versus tectonics in the Argentera Massif (French-Italian Alps). *Geomorphology,* 98(3-4), 253-266. https://doi.org/10.1016/j.geomorph.2007.10.009
54. Richards, A. Argles, T. Harris, N. Parrish, R. Ahmad, T.Darbyshire, F. & Draganits, E. (2005) Himalayan architecture constrained by isotopic tracers from clastic sediments: Earth Planet. *Science Letters*, 236, 773–796.41. https://doi.org/10.1016/j.epsl.2005.05.034
55. Royden, L. H., Burchfiel, B. C., King, R. W., Wang, E., Chen, Z., Shen, F. & Liu, Y. (1997). Surface deformation and lower crustal flow in eastern Tibet. *Science,* 276 (5313), 788–790. https://doi.org/10.1126/science.276.5313.788.
56. Schumm, S. A. (1956). Evolution of drainage systems and slopes in badlands at Perth Amboy, New Jersey. *Geol. Soc. Am. Bull.,* 67, 597-646.
57. Schumm, S.A., Dumont, J.F. & Holbrook, J.M. (2002). Active tectonics and alluvial rivers: Cambridge University Press, *Cambridge,* 276. ISBN: 0 521 66110 2.
58. Seeber, L. & Armbruster, J. (1981). Great detachment earthquakes along the Himalayan Arc and long-term forecasting. In D. W. Simpson & P. G. Richards (Eds.), Earthquake prediction: An international review. *Maurice Ewing Series*, 4, 259–277.
59. Seeber, L. & Gornitz, V. (1983). River profiles along the Himalayan arc as indicators of active tectonics. *Tectonophysics*, 92(4), 335- 367. https://doi.org/10.1016/0040-1951(83)90201-9
60. Silva, P.G., Goy, J.L., Zazo, C. & Bardajm, T. (2003). Fault-generated mountain fronts in southeast Spain: Geomorphologic assessment of tectonic and seismic activity. *Geomorphology*, 50(1-3), 203-225.43. https://doi.org/10.1016/S0169-555X(02)00215-5
61. Smith, K. G. (1950). Standards for grading texture of erosional topography. *American Journal of Science*, 248 (9), 655-668.
62. Srivastava, P. & Mitra, G. (1994). Thrust geometries and deep structure of the outer and inner Lesser Himalaya, Kumaun and Garhwal (India): Implications for evolution of the Himalayan fold and thrust belt. *Tectonics*, 13(1), 89109. https://doi.org/10.1029/93TC01130
63. Strahler, A. N. (1952). Hypsometric (area-altitude) analysis of erosional topography. *Geological Society of America Bulletin*, 63(11), 1117–1142.

64. Strahler, A. N. (1957). Quantitative analysis of watershed geomorphology. Eos, *Transactions American Geophysical Union*, 38(6), 913-920.
65. Strahler, A. N. (1964). Quantitative geomorphology of drainage basins and channel networks. In:V. T. Chow (ed), Handbook of applied hydrology. *McGrawHill Book Company*, New York, section 4-II.
66. Tapponnier, P., Zhiqin, X., Roger, F., Meyer, B., Arnaud, N., Wittlinger, G. & Jingsui, Y. (2001). Oblique stepwise rise and growth of the Tibet Plateau. *Science,* 294 (5547), 1671-1677. https://doi.org/10.1126/science.105978
67. Thakur, V. C. (2004). Active ectonics of himalayan frontal thrust and seismic hazard to ganga plain. *Current Science*, 86 (11), 1554-1560.
68. Thomson, N. R. & Clilverd, M. A. (2001). Solar flare induced ionospheric D-region enhancements from VLF amplitude observations. *Journal of Atmospheric and Solar-Terrestrial Physics*, 63(16), 1729-1737. https://doi.org/10.1016/S1364-6826(01)00048-2
69. Valdiya, K. S. (1980a). Geology of the Kumaun Lesser Himalaya: Dehra Dun, India, *Wadia Institute of Himalayan Geology*, p. 291.
70. Valdiya, K. S. (1980b). The two intracrustal structural levels in the Lesser Himalayan Sequence and their tectonic significance. Wadia Institute of Himalayan Geology, Dehradun, India.
71. Valdiya, K. S. (2001). Reactivation of terrane-defining boundary thrusts in central sector of the Himalaya: Implications. *Current Science*, 81(11), 1418–1431.
72. Valdiya, K. S. (2010). The making of India: Geodynamic evolution. New Delhi, *Macmillan Publishers India Ltd.* 816. ISBN: 0230-32833-4.
73. Valdiya, K.S., Joshi, D.D., Sanwal, R. & Tandon, S.K. (1984). Geomorphological development across the active main boundary thrust: an example from the Nainital Hills in Kumaun Himalaya, *J. Geol. Soc. India*, 25, 761-774.
74. Yeats, R.S., Sieh, K. & Allen, C.R. (1997). Geology of earthquakes, *Oxford University Press*, 568.